A Cluster Approach for the modelling of the layer-by-layer growth of SiC polytypes

Gerard L. Vignoles, Laurent Ducasse

A Cluster approach for the modelling of the layer-by-layer growth of SiC polytypes

G. L. VIGNOLES
Laboratoire des Composites ThermoStructuraux
3,Allée La Boëtie – Université Bordeaux 1
F33600 PESSAC, France
vinhola@lcts.u-bordeaux1.fr

and

L. DUCASSE,
Institut des Sciences Moléculaires
351 Cours de la Libération – Université Bordeaux 1
F33410 TALENCE Cedex, France
l.ducasse@ism.u-bordeaux1.fr

Published in
J. Phys. Chem., vol. **99** (1995), pp. 5402-5412.

A CLUSTER APPROACH FOR THE MODELLING OF THE LAYER-BY-LAYER GROWTH MECHANISM OF SiC POLYTYPES.

ABSTRACT.

A cluster approach has been designed in order to confirm the physical bases of a previously presented dynamical model for CVD-CVI SiC growth [1]. The clusters consist of two or three Si-C bilayers ; the relaxation of the bond lengths in the upper bilayer of the clusters simulates the impingement of a new bilayer on the crystal surface. The quantities relevant to the model (energies and optimized geometries) have been calculated at the semi-empirical level. The use of regular series of clusters allowed to obtain extrapolated values for infinite surfaces. Qualitative agreement has been obtained between the cluster calculations and the assumptions made for the dynamical model.

INTRODUCTION.

Silicon carbide is known to exist under a very wide variety of polytypic forms (more than 250) [2-6]. Polytypes may be described as stacking sequences of Si-C bilayers along a particular direction, and there exists between each layer two alternative orientations, referred to as **h** and **k**. In addition to short and long-period polytypes of SiC [7-8], there also exists the so-called "one-dimensionally disordered" ones [9-11], which may be obtained by means of the Chemical Vapor Deposition (CVD) or Infiltration (CVI) process [12-14]. A recent contribution [1] has proposed a model accounting simultaneously for the occurrence of *both* ordered and disordered polytypes in far-from-equilibrium processes, based on an iterative scheme giving, from the

deformations of the surface bilayer, the orientation and the deformations of the new bilayer.

Confirmation and extension of this new model require a better knowledge of the interatomic interactions giving rise to polytype growth. Quantum chemical calculations might give accurate insights on such interactions in SiC. Two routes are feasible to study the electronic properties of the solid. First, one may calculate the wavefunction of a periodic system using band structure approach and Bloch functions. Second, it is possible to calculate the properties of clusters of increasing size and extrapolate to the properties of the infinite system. In this paper, we have retained the cluster approach. Moreover, in order to describe properly the crystal surface, it is necessary to manage clusters of large size. Consequently, semi-empirical techniques have been used.

The core of the clusters were made of several Si-C bilayers, and the bond lengths in the upper bilayer are allowed to relax, thus simulating the impingement of a new bilayer on the crystal surface, and reproducing the main feature of a layer-by-layer growth situation.

After a rapid description of the crystallographic aspects of silicon carbide polytypism, the physical bases of the dynamical model are reviewed. The features of the cluster approach are then described in detail, followed by the presentation of the results. The last part of the paper provides a discussion of the results in front of the assumptions taken for the dynamical model.

1. DESCRIPTION OF SILICON CARBIDE POLYTYPISM.

Silicon carbide polytypes may be described as different stacking sequences of SiC layers along a $<111>_\beta$ or the $[0001]_\alpha$ direction of the corresponding cubic or hexagonal structures [9,15], which are also the only growth directions of interest to control polytypism [2,3,16,17]. Each layer actually

consists of two sublayers, one of pure Si and the other of pure C, both in a hexagonal arrangement [15]. A schematic representation is shown in Fig.1. During the growth process, every new layer may stack in two possible positions : it is either a continuation of the former orientation, plus a translation (orientation **k**), or is in the symmetrical orientation, with both translation and 180° rotation (orientation **h**) [5,9]. As it is apparent from Fig.1, these two orientations lead to unequivalent atomic neighborhoods: if the new layer has **h** orientation, the atoms of its upper sublayer are in eclipsed conformation with respect to the atoms of the lower sublayer of the preceding layer, *i. e.*, their third neighbors along the growth axis, while in **k** orientation, they are staggered [18]. Each polytype, ordered or not, can be described by an *orientation sequence* U_n, n being the integer layer index. U_n is a BOOLEAN sequence [1].

All polytypes, except the purely cubic structures, exhibit deviations from their associated ideal structure. The coordination tetrahedra of every atom can be distorted along the <111> direction, usually retaining its threefold symmetry axis parallel to it [18]. The bond lengths have been reported to vary always by less than 3% from ideal ones, and the angles by lesser amounts [18,19].

Three geometrical variables (assuming there are no specific surface modifications due to dangling bonds rearrangements) characterize each bilayer : the length L_n of the Si-C bond parallel to the growth axis; the length l_n of the three remaining Si-C bonds and the angle A_n between L_n and l_n, as shown in Fig. 1. If each layer is in epitaxial relation with the preceding one, the **a** parameter of the equivalent hexagonal unit cell is constant and equal to $3/2\ l_n\ sin(A_n)$. This implies that only one of the two variables l_n and A_n has to be considered ; therefore, A_n has been further considered constant and ideal.

2. THE ITERATIVE MODEL.

At CVI temperatures (~1300 K), *i. e.* far below the decomposition point of SiC (~2800 K), most of the growing crystal is not able to rearrange itself : this is why the growth occurs far from *global* equilibrium. The growth mechanism is roughly depicted in Figs. 2a-c) : when a new bilayer arrives onto the surface (fig. 2a)), it has not already a bulk-like configuration and no specific relative orientation. When it gets "stuck" to the surface (fig. 2b)), it begins to relax, but its upper atoms may "oscillate" some time before choosing the most energetically favored position. Then, it completes relaxation (fig. 2c)) and is considered as "frozen" with respect to the incoming bilayers.

A simplified view of the mechanism has been used, since it is not possible to handle all the degrees of freedom displayed by a bilayer in the above scheme. We rely rather on a *local* equilibrium hypothesis, described in figs. 2d-f). The surface is considered to be represented by the atoms of the last layer, of index n. As the **a** parameter is fixed, the layer is characterized by only two independent variables, *e. g.* l_n and L_n. Let then come from an infinite distance the (bare) Si and C atoms that are going to form the next bilayer, supposed to be already in a bulk-like arrangement for sake of simplicity (fig. 2d)). At this point, the orientation choice appears : the atoms of the upper layer may lie exactly over their third neighbors (**h**, or eclipsed), or exactly over the barycenter of triplets of them (**k**, or staggered) (fig. 2e)). The proper energetic calculations (*i. e.* including third-neighbor interactions) are performed in both cases by allowing only the relaxation of impinging atoms. Two different energy values, $E_{n+1,\mathbf{h}}$ and $E_{n+1,\mathbf{k}}$, are calculated, and the lowest of them is retained as the effective E_{n+1} (fig. 2f)). The corresponding orientation is then U_{n+1}, and the corresponding lengths are l_{n+1} and L_{n+1}, from which the whole procedure may be iterated to determine U_{n+2}, l_{n+2} and

L_{n+2}, and so on... The growth is thus described by the repetition of a calculation using l_n and L_n to evaluate U_{n+1}, l_{n+1} and L_{n+1}. Vignoles [1] has built a recurrence law based on bond lengths computed by means of *ab initio* pseudopotential simulations for several simple polytypes [19], the results of which are coherent with the few existing XRD measures [20,21,18] and the ^{29}Si MAS NMR spectra of these polytypes [20-25]. However, many questions remain unanswered. First, these simulations and measures have been carried on bulk structures of these polytypes, while our modelization is aimed at describing the production of polytypic forms during the growth. Second, the number of available values for bilayer deformations is very small, while a better knowledge of the recurrence law giving the deformations and orientation of the new bilayer on the preceding one requires a much larger amount of data. Third, our model implies that the difference between the energies of the forms **h** and **k** determines the choice between these forms, but it remains to be shown that this difference actually exists and depends on the geometry of the former layer. Last, the role of control parameters such as pressure and temperature has to be investigated. The simulations on clusters have been performed to clarify these points.

3. METHODOLOGY OF THE CLUSTER STUDY.

Each cluster consists of a silicon carbide core surrounded by hydrogens in order to satisfy the valences of the peripheral silicon and carbon atoms. The SiC core includes two or three bilayers stacked on each other : the upper one represents the new bilayer that still has a choice in orientation, and the lower ones represent the <111> surface of the SiC crystal. According to the local thermodynamical equilibrium hypothesis (here restricted to the new layer), total energy calculations have been carried out on these clusters with the new bilayer in **h** and in **k**, and allowing its atoms to relax following the possible degrees of freedom in the bulk crystal. For sake of simplicity, no

surface reconstruction has been taken into account. The obtained values are :

– Relaxation energies for similar clusters differing only by the orientation of the new bilayer,

– Interatomic bond lengths after relaxation.

These quantities have been studied as functions of the interatomic distances of the lower bilayers, thus allowing to determine whether the interatomic distances (and consequently the relative deformations of the bilayers) are critical for the energetic choice between both possible orientations of the new bilayers during growth, and how they act inside a dynamical bilayer stacking model.

3.a) Calculation method.

The studied clusters contain 14 to 98 heavy atoms, *i. e.* Si and C atoms. The sizes of the two largest ones are approximately 23×14.5×5.5 $Å^3$ and 17×11.5×8.5 $Å^3$. Because of their important number of atoms, it is not possible to use performing enough *ab initio* methods. We use instead semi-empirical methods where the integrals corresponding to the Hamiltonian overlap and bielectronic terms are tabulated. These methods are known to give quite generally reliable values for the optimized geometries of the molecules. In many cases, the results are much better than the corresponding ones obtained with an *ab initio* calculation performed with small or medium size quality basis sets. Calculations were carried using the AMPAC software version 4.0 [26] installed at CIRCE and adapted by D. LIOTARD, from the Laboratoire de Physico-Chimie Théorique of the University of Bordeaux I. This software has been tested by comparison with a strictly *ab-initio* one (GAUSSIAN 92 [27]) and with experimental values determined by electron diffraction spectroscopy [28] on the $H_3Si–CH_3$

molecule in eclipsed and staggered conformations, and optimizing all interatomic distances. As the CH_3 and SiH_3 groups rotate freely at 300 K, the given experimental values correspond to both conformations.

Table 1 compares the results obtained using AMPAC and GAUSSIAN 92 with two different sets of atomic orbitals, for interatomic distances after relaxation, differences of heats of formation, and the electronic charges born by each atom. It can be readily seen that the charges on Si and C, as well as the Si-C distance, are too large according to GAUSSIAN 92 : indeed, this approach sees the molecule as being too polarized ; however, increasing the number of AOs in the basis (*e. g.*, from a 3-21G to a 4-21G basis set) makes these quantities tend towards more realistic values.

3.b) Geometry of the clusters.

The competition between **h** and **k** orientations is modelized by calculating the energies of pairs of clusters with identical numbers of atoms, one with the new bilayer in **h** orientation and one in **k**. Two-bilayer clusters have been used, for which regular series with enough terms have been established. The extrapolation to infinite of these series allows to obtain the most pertinent values for geometrical and energetical quantities. Three-bilayer clusters were also studied, but the limitation imposed by the software possibilities on the number of atoms precludes a reliable extrapolation. Figure 3 shows an example of two-bilayer clusters.

The geometry of the clusters obeys certain constraints :

– All the valences are satisfied by bonding peripheral heavy atoms to H atoms (the ratio of H to heavy atom is close to 1, due to the reduced size of the clusters) : the presence of dangling bonds would affect considerably the electronic states and the local geometry of the heavy atoms.

– In order to compare directly the **h** and **k** forms of the clusters, they must display the same number of atoms and the same number of inter-bilayer bonds.

3.c) Observed quantities.

In order to follow rigorously the conventions of the previous section, three bilayers at least are needed to define the interlayer distances L_n and L_{n+1}, as well as the intralayer distances l_n and l_{n+1} (neither l_{n-1}, nor U_n are considered, as they are not necessary to the minimal model). However, since variations of L_n imply differences in 4$^{\underline{th}}$-neighbor interactions or upper, this quantity does not play *a priori* as important a role as l_n. Consequently, calculations made with two bilayers only are also relevant : in this case, L_n is not defined, but its absence is compensated by the fact that the series of calculable clusters is larger.

$E_{n+1,\mathbf{h}}$ and $E_{n+1,\mathbf{k}}$ are the heats of formation of the hexagonal and cubic clusters, after relaxation of the Si and C layers constituting the upper bilayer. These quantities represent the differences between the total energy of each cluster and the energy of the constitutive atoms set at an infinite distance from each other. Therefore, the heats of formation for the two orientations are directly comparable, provided the two clusters have the same numbers of atoms and bonds. The quantity used to compare two clusters of different sizes is the ratio between their heats of formation and the number of Si-C pairs present in the upper bilayer, since they are the only ones involved in the difference between **h** and **k**. However, this quantity implicitly includes the presence of peripheral hydrogens ; accordingly, it will be expected to vary with the cluster size, since there are less hydrogens per heavy atom in a large cluster than in a small one.

The computed total energies are sums of a negative energy contribution from the electrons and a positive term from core-core repulsion. Their magnitude are about -250 eV per Si-C pair, a value consistent with the data reported in [19]. The differences between **h** and **k** are roughly 20 meV/Si-C pair, also consistent with the same authors. It should be pointed out that, if this difference is only 0.01% of the total energy, it represents also 2 to 3% of the heat of formation and is thus no more negligible.

To keep coherence with the dynamical model presented above, the relaxations have been allowed only along the growth direction, because it is the only direction associated to the degrees of freedom for the atomic displacements in the bulk solid and also the only direction of interest in the study of SiC polytypism. Many degrees of freedom have been forgotten, which correspond to possible surface reconstructions or contraction effects due to the finite size of the clusters. This important limitation is not very realistic, as one aims to describe the growth of a crystal. However, our model takes into account the two most important geometrical variables.

The energy and relaxation parameters of a cluster are evaluated according to the following procedure :

– An "ideal" initial geometry is first determined for the cluster, where all bond angles have the ideal value of 109°28'.

– The lengths L_{n+1} et l_{n+1} are relaxed, while all the atomic positions of the lower bilayers are kept frozen, as well as the transversal crystallographic parameter **a** (epitaxy condition). After minimization of the total energy (*i. e.*, once the local thermodynamical equilibrium condition is satisfied), one obtains simultaneously the interatomic bond lengths for the new bilayer and the heat of formation E_{n+1} of the cluster.

For pairs of clusters in **h** and **k** orientations, the energies $E_{n+1,\mathbf{h}}$ and $E_{n+1,\mathbf{k}}$ as well as the deformations $l_{n+1,\mathbf{h}}$, $l_{n+1,\mathbf{k}}$, $L_{n+1,\mathbf{h}}$ and $L_{n+1,\mathbf{k}}$ have been calculated for given values of L_n, l_n, and **a**.

4. RESULTS OF THE CLUSTER APPROACH.

4.1 – Influence of cluster size.

4.1.a) Evolution of the energy difference between h and k.

The heats of formation in **h** and **k** have been computed for a great number of clusters, with parameters l_n, L_n, and $\mathbf{a}\sqrt{6}/4$ set all equal to 1.87 Å, leaving thus ideal values for the bond angles in all the lower bilayers. Fig 4a) shows that the absolute value of the heat of formation per mole of SiC increases with the number of atoms. It is clear that the data corresponding to different numbers of bilayers define different series of slowly convergent values. However, for 49 atoms per bilayer, convergence has not yet been achieved towards a limiting value which would represent the true solid, thus showing the limitation of the cluster approach.

Fig. 4b) is a plot of the difference $\Delta E = E_{n+1,\mathbf{h}} - E_{n+1,\mathbf{k}}$ versus size. This difference is always positive in our convention (so **k** is preferred to **h**), but it tends to vanish with increasing size.

4.1.b) Extrapolation from a regular series of clusters.

If a global qualitative trend is recognized from figs. 4a) and b), it is not possible to guess more precisely what occurs if the size tends towards infinite. Figure 4b) shows that the results are scattered, mainly because of the variety in the forms of the clusters - some are "long" ones and others are more round-shaped, etc.... However, it is possible to select certain clusters that form regular series with constant global shape and increasing size. The most interesting of these suites is formed by the losange-shaped clusters

described at table 2. For two bilayers, the 4 first terms of the series were small enough to allow computations with our version of AMPAC, while for three bilayers, the first three terms only have been used.

Three quantities are of interest to describe the evolution of these clusters towards solid state : (i) the number of Si-C pairs per bilayer, which is a measure of the <111> surface, (ii) the ratio H/SiC between the number of hydrogens and the number of Si-C pairs, ad (iii) the ratio B/SiC between the number of Si-C bonds and the number of Si-C pairs in the upper bilayer (this ratio should in all cases be strictly inferior to 4 since it involves non-bulk atoms).

The recurrence law giving the number of Si-C pairs per bilayer as a function of the index i of the series is easy to reach from table 2. If N_i is that quantity and N_1, N_2, N_3 and N_4 its first terms, it is readily seen that the successive differences $\Delta_i = N_i - N_{i-1}$ are 5, 7, 9, that is, $5 + (i-2)\times 2$; therefore the recurrence law is :

$$N_i = N_{i-1} + 5 + (i-2)\times 2 \qquad (1)$$

Summation of all terms over i yields a general expression for N_i :

$$N_i = N_1 + 5(i-1) + \frac{(i-1)(i-2)}{2}\times 2 \qquad (2)$$

and, with $N_1 = 3.5$:

$$N_i = 0.5 + 2i + i^2 \qquad (3)$$

One shows similarly that the number of peripheral hydrogens H_i and the number of bonds B_i obey the following laws :

$$H_i = 10 + 8i + i^2 \qquad (4)$$

$$\text{and} \quad B_i = 9 + 12i + 3.5i^2 \tag{5}$$

Expressions (3), (4) and (5) allow to determine the limiting values, for infinite i, of the ratios H/SiC and B/SiC :

$$\left(\frac{H}{SiC}\right)_\infty = \lim_{i\to\infty}\frac{H_i}{N_i} = \frac{i^2}{i^2} = 1$$

$$\left(\frac{B}{SiC}\right)_\infty = \lim_{i\to\infty}\frac{B_i}{N_i} = \frac{3{,}5i^2}{i^2} = 3.5$$

The value of B/SiC for the fourth term in table 2 is 3.122, which is still far from the limiting value, but now the fact of having a regular series will compensate this imperfection.

Fig. 5 is a plot of the *absolute* energetic difference ΔE_i between **h** and **k** versus the series index i. The values obtained for the first four terms strongly suggest that ΔE_i follows a second-order polynomial evolution law. Indeed, a curve fit has been made, with a negligible error. The obtained analytic expression $\Delta E_i \equiv A + Bi + Ci^2$ is further used for extrapolation towards infinite.

As N_i is also given by a second-order polynomial law in i, the energetic difference related to the number of Si-C pairs, *i.e.*, the ratio $\Delta E_i/N_i$ tends to be, as i increases, the ratio between the highest-order terms :

$$\frac{\Delta E}{SiC} = \lim_{i\to\infty}\left(\frac{\Delta E_i}{N_i}\right) = \frac{2.8820i^2}{i^2} = 2.8820 \text{ kJ/mol SiC.}$$

The very small error in the regression (roughly 0.1%) allows us to use systematically this method in the following parts of the work. First, it may be applied to the series of three-bilayer clusters. The small number of available terms suppresses any control of the error, but since the behavior of the

series looks to be very close to the preceding one (see fig. 5), the results may have some sense.

In this case, one finds a limiting value ΔE/SiC of 1.8643 kJ/mole SiC, which is notably lower. An interpretation for this fact is that the third layer (*i. e.*, the second below the surface) plays a non-negligible role in the choice of orientation for the new layer, and that its presence lowers the energetic difference between **h** and **k**.

4.1.c) Evolution of the bond lengths L_{n+1} and l_{n+1}.

Figures 6a) and b) show respectively the evolution of L_{n+1} and l_{n+1} for the regular series of two-bilayer clusters with orientations **h** and **k**. These lengths appear very neatly to tend asymptotically towards a limit. In order to estimate these limiting values, it has been tried to use interpolation functions with as few parameters as possible, and fitting correctly these evolutions. The retained formulas are the following ones :

$$L_{n+1} \text{ or } l_{n+1} \equiv A + \frac{B}{i} + \frac{C}{i^2} \qquad (6)$$

$$L_{n+1} \text{ or } l_{n+1} \equiv A + \frac{B}{i+C} \qquad (7)$$

Both cases use three parameters, the most important of which is A, since it is the limiting value for the lengths when *i* goes to infinite. Both regressions give very similar results, and the data obtained with the best reliability factors are collected in table 3a), and the corresponding plots are shown at figures 6a) and b).

As for the absolute energy differences, the regression has been applied to the three-bilayer clusters, yielding limit values close to the former ones : L_{n+1} increases by an amount of 10^{-3} Å, and l_{n+1} remains almost unchanged.

The values of l_{n+1} and L_{n+1} are such that the relative deformation, defined in [1] as $\delta_{n+1} = (L_{n+1} - l_{n+1})/L_{n+1}$, is indeed positive. Its magnitude is more or less 0.6 % in **k** and 1.0 % in **h**, slightly higher than the data from [19]. Moreover, if L_{n+1} decreases rather quickly as the cluster size increases, l_{n+1} is not much affected ; consequently δ_{n+1} also decreases and tend yet to be closer to the values reported in [1].

As a summary, increasing the surface of the clusters provokes :

– a slight increase of l_{n+1},

– a decrease of L_{n+1},

– a decrease of δ_{n+1},

– a decrease of the energetic difference between **h** et **k** (**k** becomes less preferred).

Increasing the number of bilayers provokes :

– a small increase of L_{n+1} and an even smaller one of l_{n+1},

– a neat decrease of the energetic difference between **h** et **k** (**k** becomes less preferred).

These first results seem to show, if they are crudely interpreted, that the **k** orientation is always energetically preferred to **h**. This has been claimed by several authors, either from experimental [29-31] or theoretical [32,33] bases, although the great abundance of disordered polytypes in CVD or CVI SiC deposits tends to negate this fact. However, it may readily be seen that increasing the surface or the depth of the clusters - that is, getting closer to the solid – makes the **h** and **k** forms closer in energy, possibly so close that a perturbation arising from deformations in the lower bilayers might invert the preference.

4.2 – Influence of the cell parameter a.

The XRD analyses [20,21], as well as the relaxation calculations on unit cells of bulk materials [19], show that parameter **a** (in hexagonal convention) vary from one structure to another. It is then relevant to study its influence on the heats of formation of bilayers in **h** and in **k**. Indeed, it may be a critical parameter to monitor the evolution from the dynamical production of one polytype to another. Increasing **a** indeed simulates roughly a diminution of the pressure or an increase of the temperature of the substrate.

The influence of **a** has been studied on the series of two-bilayer clusters, with l_n set to 1.87 Å. The results are shown at figures 7 and 8.

The total heats of formation $E_{n+1,\mathbf{h}}$ and $E_{n+1,\mathbf{k}}$ vary as a second-order polynomial function of the cell parameter, as it may readily be seen at figure 7a), but their difference varies linearly, with a strong positive slope (increasing **a** by 0.01 Å enhances ΔE by an amount of 0.2 kJ/mol.SiC, which represents 10% of its absolute value), as shown in figure 7b). Combining this effect with the influence of the addition of bilayers below the surface, which tends to decrease ΔE, it would lead to an inversion of the preference between **h** and **k**, in better agreement with the experimental observation.

The interatomic distances of the upper bilayer display a similar behavior in **h** and in **k**. When **a** decreases, l_{n+1} diminishes rapidly in a linear fashion (slope ~ 3/4), and L_{n+1} also diminishes linearly, though less strongly (slope ~ 1/2). The relative deformation δ_{n+1} remains positive for the investigated values, but decreases as $\mathbf{a}\sqrt{6}/4$ increases.

To summarize, an increase of **a** provokes :

– an increase of l_{n+1} and of L_{n+1} ;

– a decrease of δ_{n+1} ;

– an enhanced preference for **k**.

The cell parameter **a** influences strongly the energy difference between **h** and **k**, as well as the lengths l_{n+1} and L_{n+1} after relaxation.

4.3. Influence of l_n and L_n.

The dynamical model is based on the dependence of all the quantities of the bilayer (n+1) upon the interatomic distances of bilayer n. This fact has to be confirmed now by means of the cluster calculations.

The influence of l_n has been studied on the two-bilayer cluster series. l_n has been varied while **a** has been kept constant : accordingly, the bond angles in bilayer n are allowed to vary.

Figures 9 and 10 are plots of l_{n+1}, L_{n+1}, and $\Delta E = E_{n+1,\mathbf{h}} - E_{n+1,\mathbf{k}}$ versus l_n. The latter varies linearly with l_n ; the slope is more or less -0.05 kJ/mol SiC per 0.01 Å. This is much smaller than the corresponding variation of ΔE with **a** (0.2 kJ/mol SiC per 0.01 Å : see preceding section). The bond lengths l_{n+1} and L_{n+1} display again a similar behavior in **h** and in **k**. When l_n increases, L_{n+1} decreases strongly, and l_{n+1} does not vary significantly.

The effect of L_n has been studied on the same cluster series. It appears to be smaller than the effect of l_n. This result was expected because it is related to the interatomic interaction of atoms located at bilayers (n-1) and (n+1). Again, ΔE diminishes linearly as L_n increases (fig. 11), L_{n+1} seems to decrease slightly, and l_{n+1} is not affected (figs. 12a) and b)).

Reminding that the dynamical model presented in [1] uses a simplified recurrence only involving the deformation ratio δ_n, it could be interesting to express directly the results obtained in terms of this quantity. Indeed, when l_n decreases as L_n is fixed, or when L_n increases with a fixed l_n, the net result is

an increase of δ_n along the lines shown in the (L_n,l_n) plane of fig. 13. In this figure there is also a recall of the direction along which the values of [19] organize themselves, as interpreted by [1]. The relations between δ_{n+1} and δ_n in **h** and in **k** are shown at figures 14a) and b), in the respective cases where only L_n or l_n varies. In the case where L_n is fixed, the behavior is quasi-linear, with a positive slope of ~ 1 in **h** and ~ 0.6 in **k**, while in the converse case, the variations are much smaller. Three remarks arise :

(i) the slope of $\delta_{n+1} = f(\delta_n)$ is indeed positive, as in [1] ;

(ii) the slopes are rather steep, mainly in fig. 14a). This is a necessary condition for the production of long-period or chaotic polytypes through a recurrence law on the δ_n's ;

(iii) the behavior in **h** and **k** are distinct (neatly different slopes).

4.4 – Influence of the orientation U_n of the surface bilayer relatively to the lower one.

One simplifying assumption of the dynamical model is that U_n does not directly influence the choice of U_{n+1} ; this may be verified with two pairs of three-bilayer clusters, one pair with the middle bilayer in **h** orientation, and one pair with the middle bilayer in **k**. A computation has been performed on two three-bilayer cluster series with $L_n = l_n = \mathbf{a}\sqrt{6}/2 = 1.87$ Å. The respective values of ΔE_{n+1} are 1.864 and 1.869 for U_n = **h** and **k**, thus differing by only 0.3%. L_{n+1} and l_{n+1} differ by even smaller amounts. It may be readily seen that there is a very little influence of the orientation U_n upon all the quantities of the upper bilayer. This fact validates the approximation made in [1] by neglecting the direct influence of U_n.

CONCLUSION.

The AMPAC 4.0 software has been used to compute the heats of formations of pairs of clusters containing Si-C bilayers for which the upper

bilayer is allowed to relax in **h** or **k** orientation. The quantities required to confirm the dynamical growth model for SiC polytype generation were calculated. The relaxations have been restricted to the only ones possible in the bulk solid (respect of the epitaxy condition, all possible surface reconstructions discarded). Extrapolation of these quantities to limiting values of infinite crystal surfaces has been possible with the use of regular series of clusters. The results showed that :

– the axial deformations (*i.e.* along the growth direction) of **h** bilayers are greater than the deformations of **k** bilayers ;

– the absolute values of the deformations are in good agrement with the *ab-initio* pseudopotential calculations reported in [19] ;

– the **k** orientation looks to be always preferred to **h** on the criterion of the difference between the two heats of formation for both orientations ; however, the difference lowers with an increase of the number of bilayers contained in the clusters, and with a decrease of the transversal cell parameter **a** ;

– the deformations of the coordination tetrahedra in the surface bilayer indeed affect the energy difference between **h** and **k** for the new bilayer, as well as its deformations.

– the orientation of the surface bilayer with respect to the lower one does not affect significantly the quantities associated to the upper bilayer.

– the survey of the evolution with parameter **a** is a first step in the direction of simulating the effects of pressure and temperature on the growing surface.

The number of bilayers of the clusters on which the calculations have been made appears to be too small to allow a quantitative description of the

semi-infinite solid. However, it may be deduced from the cluster study that the energies of the new bilayer in **h** and in **k** orientations are very close to each other, and that the action of the crystallographic parameters of the surface should be enough to invert the preference for one form rather than the other. Many other decisive factors may also play a role, but the important feature is that the growth of silicon carbide can be described with a recurrence law based on bilayer deformations.

REFERENCES

[1] G. L. VIGNOLES, *J. Crystal Growth*, **118**, 430-438 (1992).

[2] "*Polymorphism and Polytypism in Crystals*", edited by A. A. Verma and P. Krishna (Wiley, New York, 1966).

[3] "*Crystal Growth and Characterization of Polytype Structure*", edited by P. Krishna, (Pergamon Press, New York, 1983).

[4] G. R. FISHER, P. BARNES, *Phil. Mag. B*, **61**, 217-236 (1990).

[5] L. S. RAMSDELL, "Studies on Silicon Carbide", **32**, 64-82 (1947).

[6] Gmelin Handbook of Chemistry, Si Suppl., **B2** (1989).

[7] T. NISHIDA, *Min. J.*, **6**, 216-239 (1971).

[8] M. YESSIK, S. SHINOZAKI, H. SATO, *Acta Cryst.*, A**31**, 764-768 (1975).

[9] H. JAGODZINSKI, *Acta Cryst.*, **2**, 201-207 (1949).

[10] S. SHINOZAKI, K. R. KINSMANN, *Acta Met.*, **26**, 769 (1978).

[11] S. SCHAMM, A. MAZEL, D. DORIGNAC, J. SEVELY, in "*Matériaux Composites pour Applications à Hautes Températures*", AMAC/CODEMAC Bordeaux 1990, edited by R. Naslain *et al.* (1990) p. 207.

[12] E. FITZER, D. HEGEN, H. STROHMEIER, *Rev. Int. Hautes Temp. Réfract.*, **17**, 23 (1980).

[13] D. P. STINTON, A. J. CAPUTO, R. A. LOWDEN, *Am. Ceram. Soc. Bull.*, **65**, 347 (1986).

[14] R. NASLAIN, F. LANGLAIS, in "*Tailoring Multiphase and Composite Ceramics*", R. E. Tressler *et al.* eds, *Mat. Sci. Res.*, **20** (1986), 145.

[15] W. F. KNIPPENBERG, *Philips Res. Rept.* **18**, 161-274 (1963).

[16] A. R. VERMA, "Crystal Growth and Dislocations" (Butterworths, London, 1953)

[17] J. CHIN, P. K. GANTZEL, R. G. HUDSON, *Thin Solid Films*, **40**, 57-72 (1977).

[18] W. WELTNER Jr., *J. Chem. Phys.*, **51**, 2469-2483 (1969).

[19] C. CHENG, V. HEINE, R. J. NEEDS, *J. Phys.: Condens. Matter*, **2**, 5115-5134 (1990).

[20] H. SCHULTZ, K. H. THIEMANN, *Solid State Comm.*, **32**, 783-785 (1979).

[21] A. H. GOMES DE MESQUITA, *Acta Cryst.*, **23**, 610 (1967).

[22] J. R. GUTH, W. T. PETUSKEY, *J. Phys. Chem.*, **91**, 5361-5364 (1987).

[23] J. S. HARTMAN, M. F. RICHARDSON, B. L. SHERRIFF, B.G. WINSBORROW, *J. Am. Chem. Soc.*, **109**, 6059-6067 (1987).

[24] D. C. APPERLEY, R. K. HARRIS, G. L. MARSHALL, D. P. THOMPSON, *J. Am. Ceram. Soc.*, **74**, 777-782 (1991).

[25] M. O'KEEFFE, *Chem. Mater.*, **3**, 332-335 (1991).

[26] AMPAC 4.0, © 1992 Semichem, 12715 W. 66th Terrace, Shawnee, KS 66216, U.S.A.

[27] GAUSSIAN 92, software produced by M. J. FRISCH, M. HEAD-GORDON, H. B. SCHLEGEL, K. RAGHAVACHARI, J. S. BINKLEY, C. GONZALEZ, D. J. DEFREES, D. J. FOX, R. A. WHITESIDE, R. SEEGER, C. F. MELIUS, J. BAKER, R. L. MARTIN, L. R. KAHN, J. J. P. STEWART, E. M. FLUDER, S. TOPIOL, J. A. POPLE, from Gaussian Inc., Pittsburgh, PA, USA (1992).

[28] A. C. BOND, L. O. BROCKWAY, *J. Am. Chem. Soc.*, **76**, 3312 (1954).

[29] N. W. JEPPS, T. F. PAGE, *Prog. Cryst. Growth Charact.*, **7**, 259-307 (1983).

[30] J. N. NESS, T. F. PAGE, *Bull. Minéral.*, **109**, 151-161 (1986).

[31] S. R. NUTT, "Defects in silicon carbide whiskers", *J. Am. Ceram. Soc.*, **67** (1984), 428-431.

[32] S. R. NUTT, F. E. WAWNER, *J. Mater. Sci.*, **20**, 1953-1961 (1985).

[33] V. HEINE, C. CHENG, R. J. NEEDS, *J. Am. Ceram. Soc.*, **74**, 2630-2633 (1991).

Table 1. Comparison of results from different numerical approaches. * from [28] ; ** from [2], about the partially ionic character of SiC.

	AMPAC 4.0	GAUSSIAN 92 (3-21G basis set)	GAUSSIAN 92 (4-21G basis set)	Experimental measures *
Eclipsed (**h**)				
Si - C distance (Å)	1.886	1.933	1.907	
Si - H distance (Å)	1.492	1.495	1.478	
C - H distance (Å)	1.092	1.082	1.084	
Charge on Si	+ 0.448 e	+ 0.899 e	+ 0.689 e	
Charge on C	- 0.278 e	- 0.858 e	- 0.793 e	
Staggered (**k**)				
Si - C distance (Å)	1.880	1.923	1.894	1.857 ± 0.007*
Si - H distance (Å)	1.492	1.495	1.478	1.48 ± 0.02*
C - H distance (Å)	1.092	1.083	1.085	1.09 ± 0.02*
Charge on Si	+ 0.449 e	+ 0.895 e	+ 0.682 e	+ 0.33**
Charge on C	- 0.277 e	- 0.846 e	- 0.778 e	- 0.33**
Difference between total energies $E_h - E_k$ (kJ/SiC pair)	5.189	4.938	6.380	

Table 2. Description of the losange-shaped clusters with two or three bilayers, corresponding to a two-dimensional growth. * Tends to 1 for infinite planes. ** Tends to 3.5 for infinite planes.

Number of atoms per bilayer and geometry	Number of Si-C pairs in the upper bilayer	Total number of H atoms in the upper bilayer	Number of Si-C bonds in the upper bilayer	Ratio H/(Si+C) pairs *	Ratio Si-C bonds/ (Si+C) pairs**
7 atoms 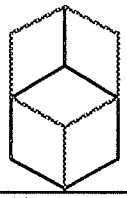	3.5	10	9	2.858	2.572
17 atoms 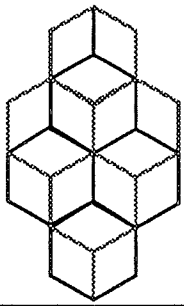	8.5	19	24.5	2.236	2.882
31 atoms 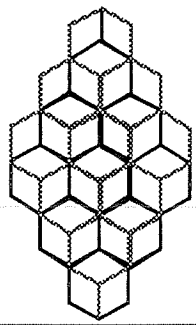	15.5	30	47	1.936	3.032
49 atoms 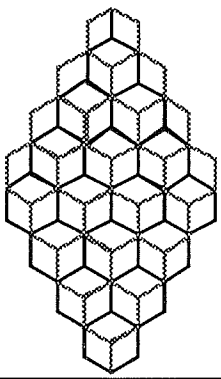	24.5	43	76.5	1.756	3.122

Table 3. Coefficients of the regressions for bond lengths L_{n+1} et l_{n+1} in **h** and in **k**, following the equations : (i) Length $\equiv \mathbf{A} + \frac{\mathbf{B}}{i} + \frac{\mathbf{C}}{i^2}$; (ii) Length $\equiv \mathbf{A} + \frac{\mathbf{B}}{i+\mathbf{C}}$. **a)** Two-bilayer clusters. R = reliability factor. **b)** Three-bilayer clusters.

	A (Å) (= limit value)	B (Å)	C	R
$L_{n+1,\mathbf{h}}$ (ii)	1.8637	-0.02066	1.2359	0.999996
$L_{n+1,\mathbf{k}}$ (i)	1.8563	0.00482	$2.32.10^{-4}$Å	0.999908
$l_{n+1,\mathbf{h}}$ (i)	1.8499	-0.00084	$1.42.10^{-5}$ Å	0.999987
$l_{n+1,\mathbf{k}}$ (i)	1.8486	-0.00455	$1.27.10^{-3}$ Å	0.999771

a)

	A (Å) (= limit value)	B (Å)	C (Å)
$L_{n+1,\mathbf{h}}$ (i)	1.8691	0.027097	-0.018333
$L_{n+1,\mathbf{k}}$ (i)	1.8603	0.011329	-0.006877
$l_{n+1,\mathbf{h}}$ (i)	1.8491	-0.001103	0.000398
$l_{n+1,\mathbf{k}}$ (i)	1.8483	-0.007973	0.005362

b)

FIGURE CAPTIONS

Fig. 1. Schematic description of a disordered SiC polytype observed along a $<11\bar{2}0>_{\alpha}$ direction.

Fig. 2. Schematic descriptions of the bilayer formation : **a,b,c)** : as it occurs in CVD ; **d,e,f)** : as modelized in this work.

Fig. 3. A pair of clusters reproducing the two possible orientations for the new layer. **a) h** orientation. **b) k** orientation.

Fig. 4. Evolution with cluster size. The clusters have two or three bilayers. $l_n = \mathbf{a}\sqrt{6}/4 = 1{,}87$ Å. **a)** Evolution of the heat of formation (per mole of Si-C atomic pairs).**b)** Evolution of the energetic difference between **h** and **k** orientations.

Fig. 5. Evolution with *i* of the absolute energetic difference between **h** and **k** for the cluster suites of Table 2.

Fig. 6. Evolution with *i* of bond lengths in the upper bilayer after relaxation. **a)** Evolution of L_{n+1}. **b)** Evolution of l_{n+1}.

Fig. 7. Variation of cell parameter **a**. The given values are extrapolated from the two-bilayer cluster series for $l_n = 1.87$ Å.**a)** Evolution of $E_{n+1,\mathbf{h}}$ and of $E_{n+1,\mathbf{k}}$. **b)** Evolution of $\Delta E = E_{n+1,\mathbf{h}} - E_{n+1,\mathbf{k}}$.

Fig. 8. Variation of the bond lengths of the upper bilayer with **a**. Values obtained by extrapolation on the two-bilayer cluster series. **a)** Variation of L_{n+1}. **b)** Variation of l_{n+1}.

Fig. 9. Influence of l_n. Two-bilayer cluster series. $\mathbf{a}\sqrt{6}/4 = 1.87$ Å. **a)** Evolution of L_{n+1}. **b)** Evolution of l_{n+1}.

Fig. 10. Evolution of the energy difference ΔE with l_n. Two-bilayer cluster series.

Fig. 11. Evolution of the difference $\Delta E = E_{n+1,\mathbf{h}} - E_{n+1,\mathbf{k}}$ with L_n. Three-bilayer cluster series. $l_n = \mathbf{a}\sqrt{6}/4 = 1.87$ Å.

Fig. 12. Evolution of the bond lengths of the upper bilayer with L_n. Three-bilayer cluster series. $l_n = a\sqrt{6}/4 = 1.87$ Å. **a)** Evolution of L_{n+1}. **b)** Evolution of l_{n+1}.

Fig. 13. Displacements in the plane (L_n,l_n) corresponding to figures 14 a) et b).The arrows indicate the direction of increasing δ_n.

Fig. 14. Relation between δ_{n+1} and δ_n in **h** and in **k**. **a)** when only l_n varies. **b)** when only L_n varies.

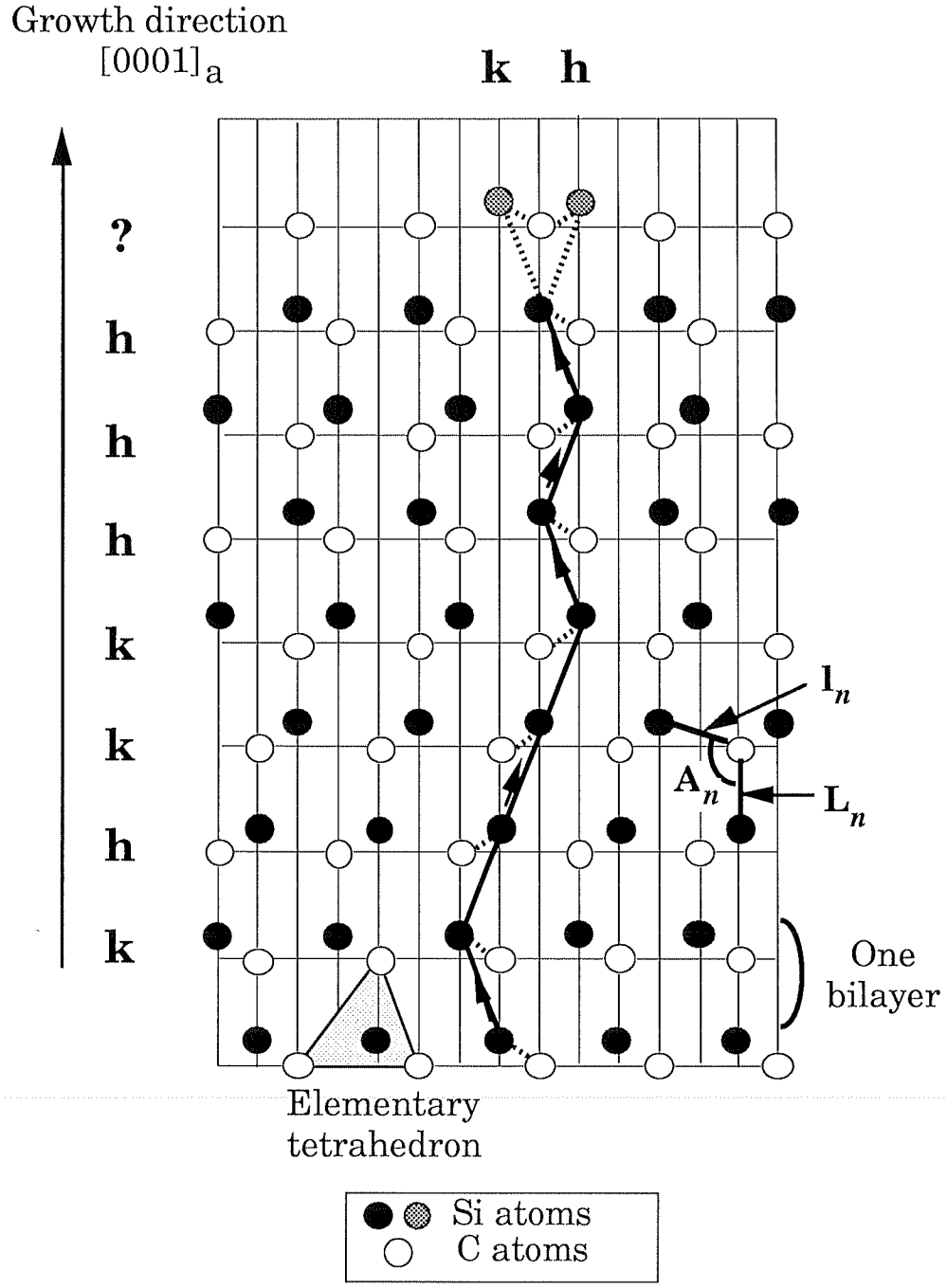
Growth direction
[0001]a
k h
?
h
h
h
k
k
h
k
l_n
A_n
L_n
One bilayer
Elementary tetrahedron
Si atoms
C atoms

Fig. 1.

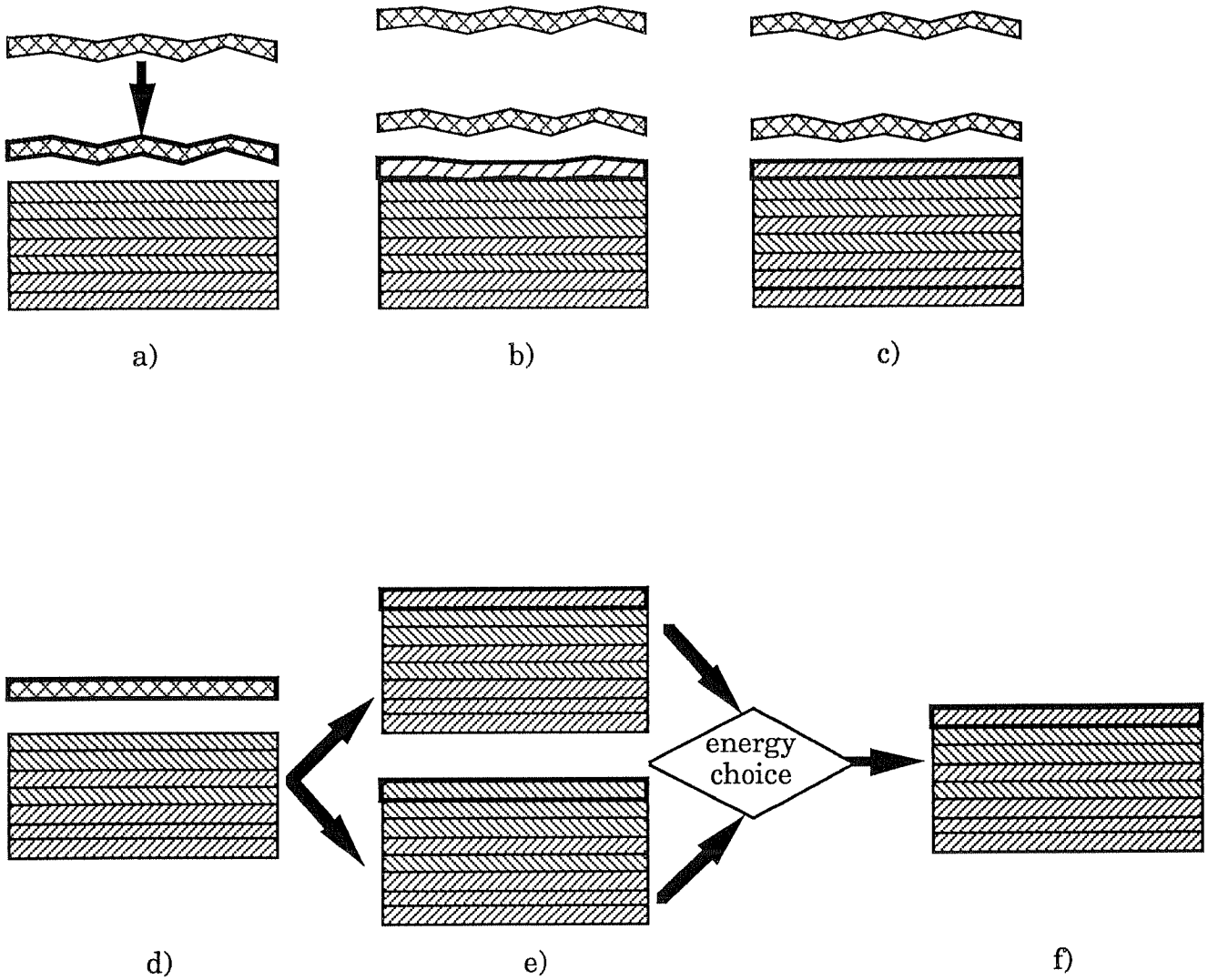

Fig. 2.

G. L. VIGNOLES & L. DUCASSE

Fig. 3.

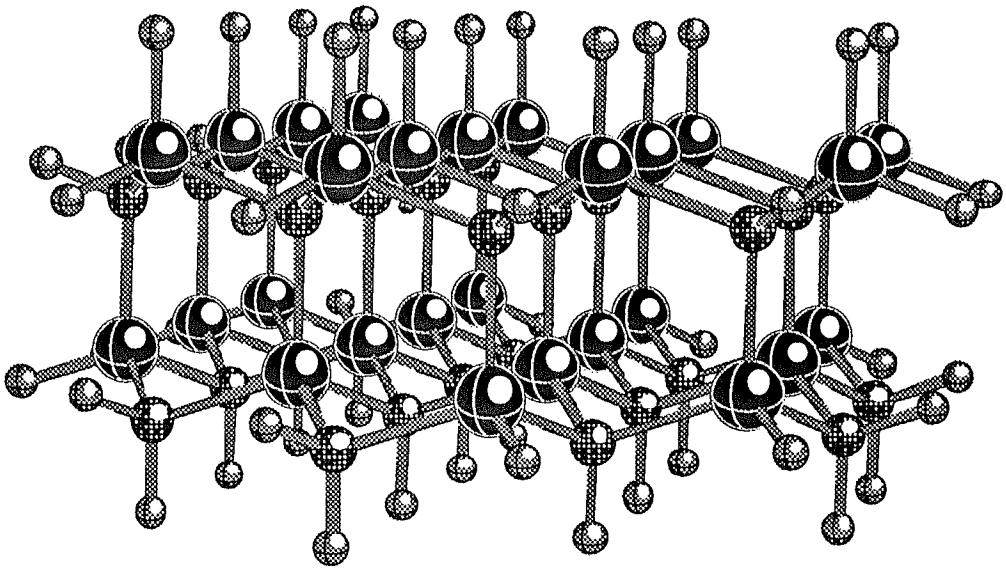

a)

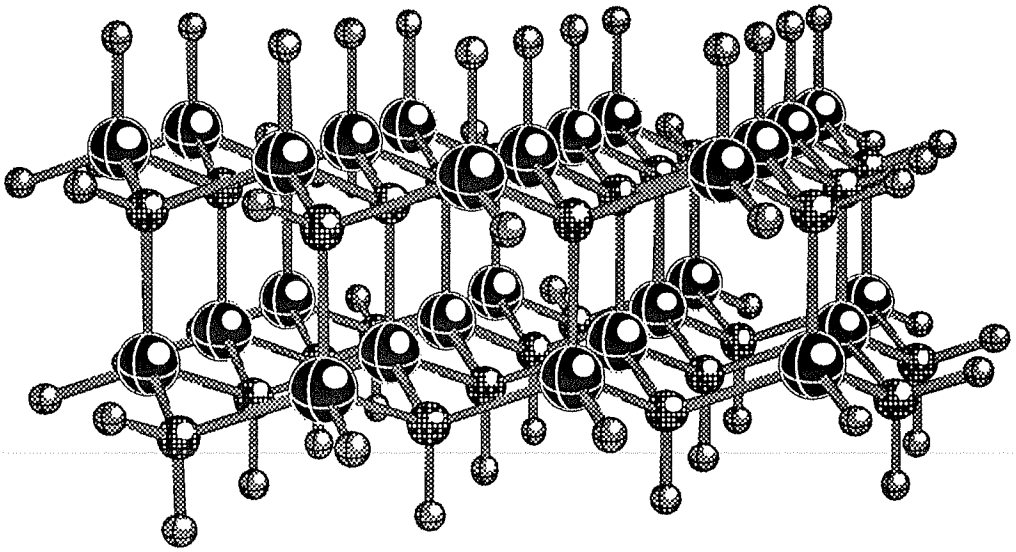

b)

Legend :

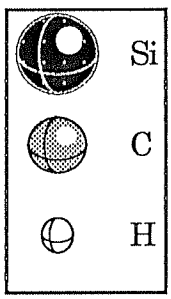

G. L. VIGNOLES & L. DUCASSE

Fig. 4.

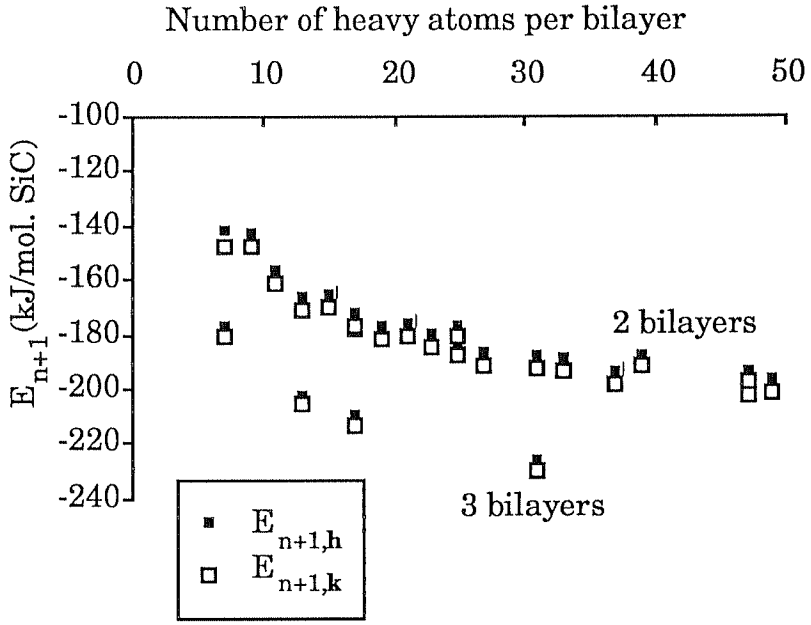

a)

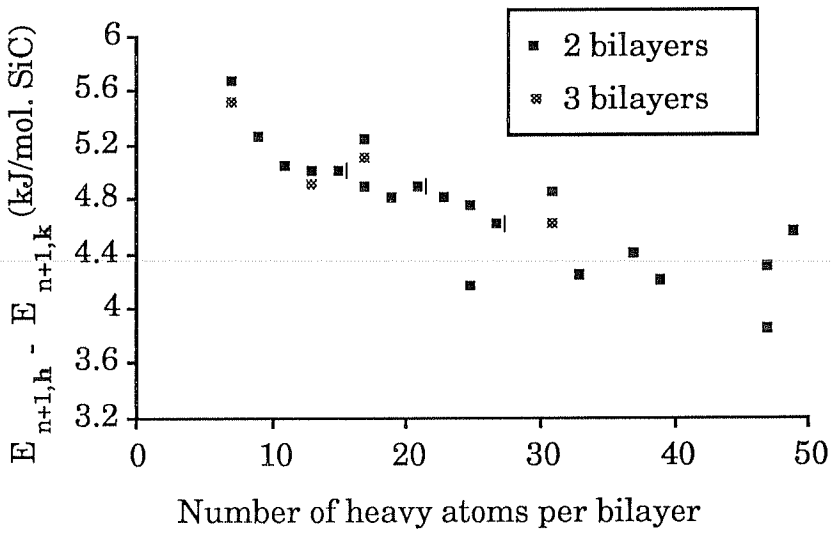

b)

G. L. VIGNOLES & L. DUCASSE

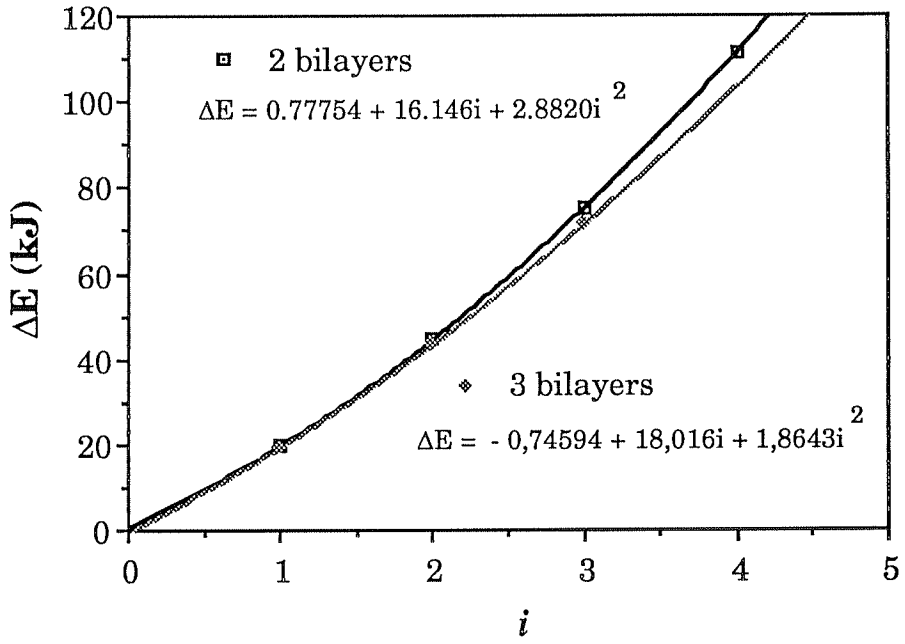

Fig. 5.

G. L. VIGNOLES & L. DUCASSE

Fig. 6.

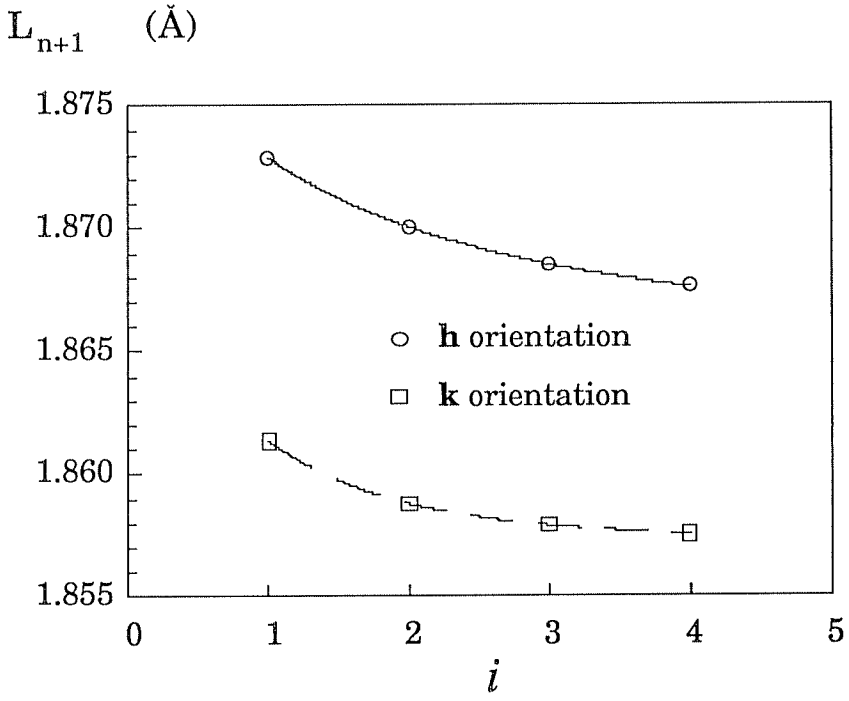

a)

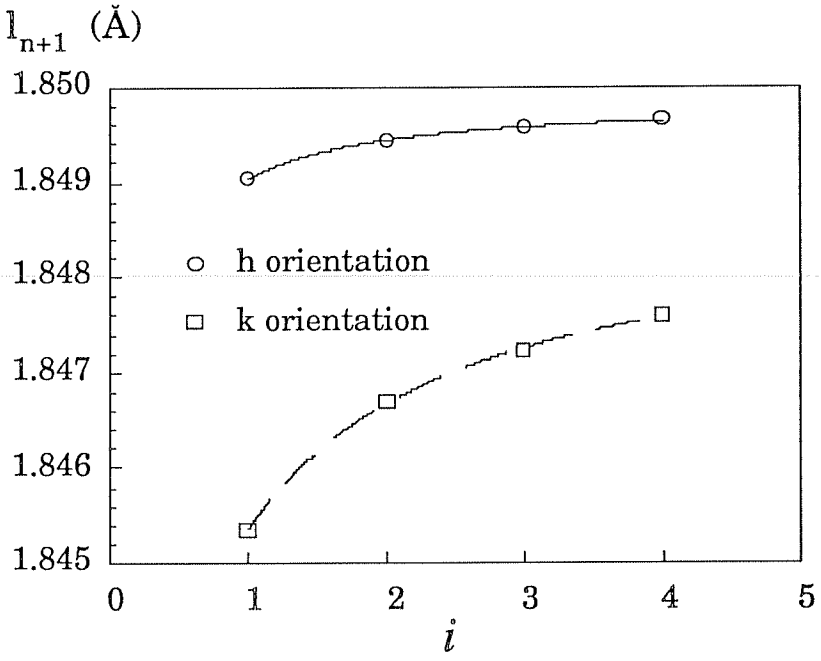

b)

G. L. VIGNOLES & L. DUCASSE

Fig. 7.

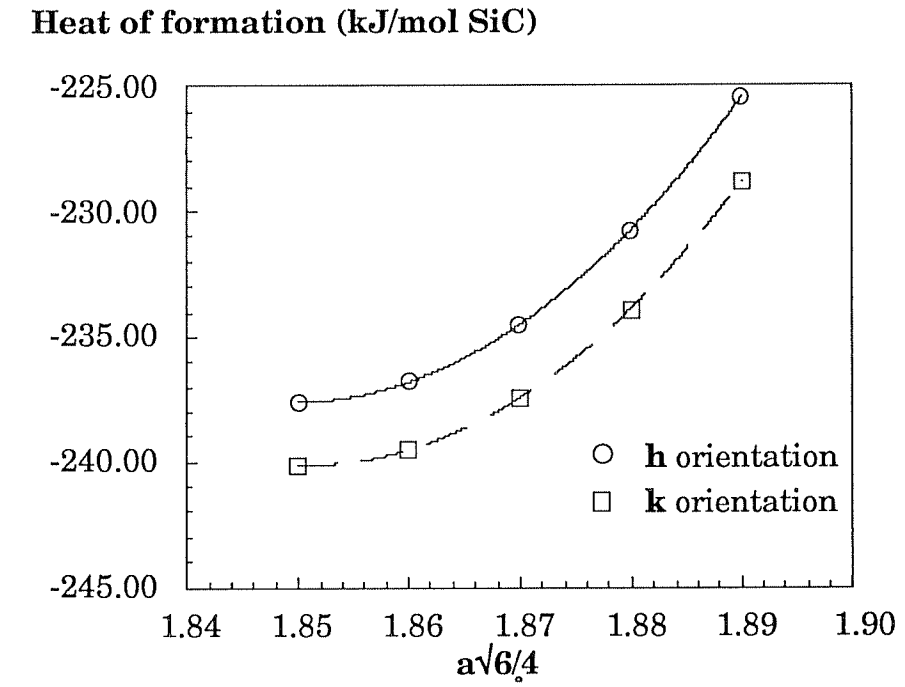

a)

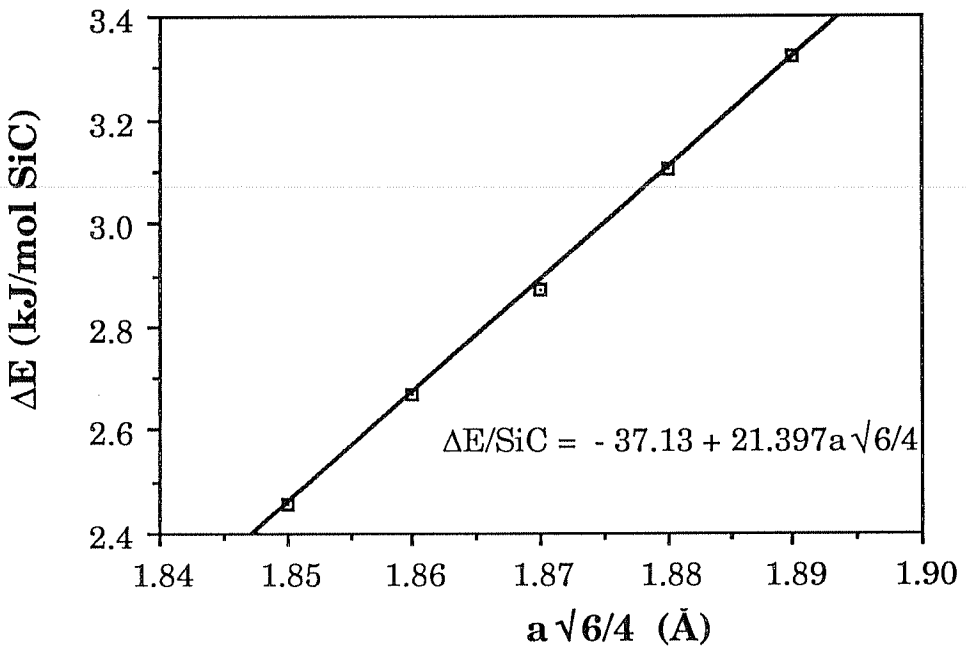

b)

G. L. JIGMOES & L. DUCASSE

Fig. 8.

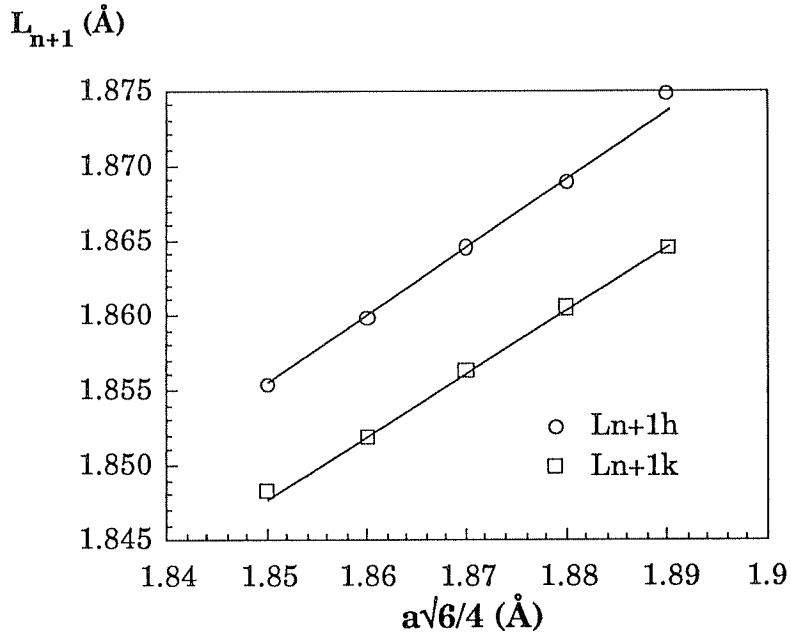

a)

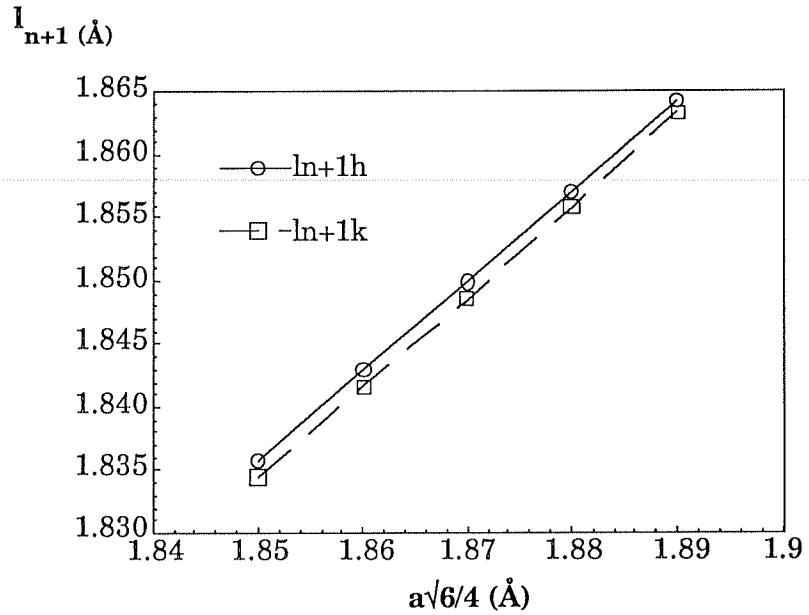

b)

G. L. VIGNOLES & L. DUCASSE

Fig. 9.

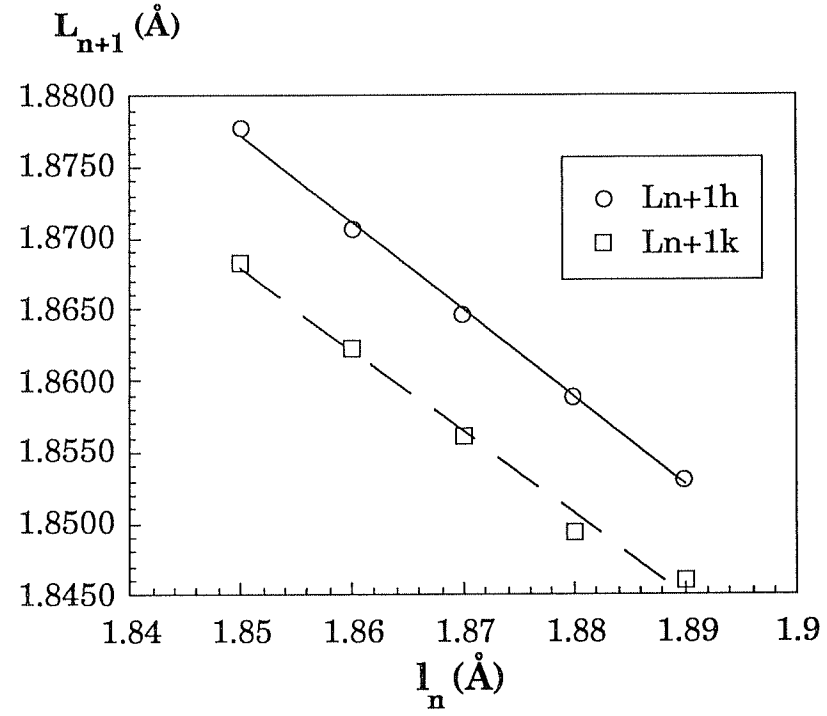

a)

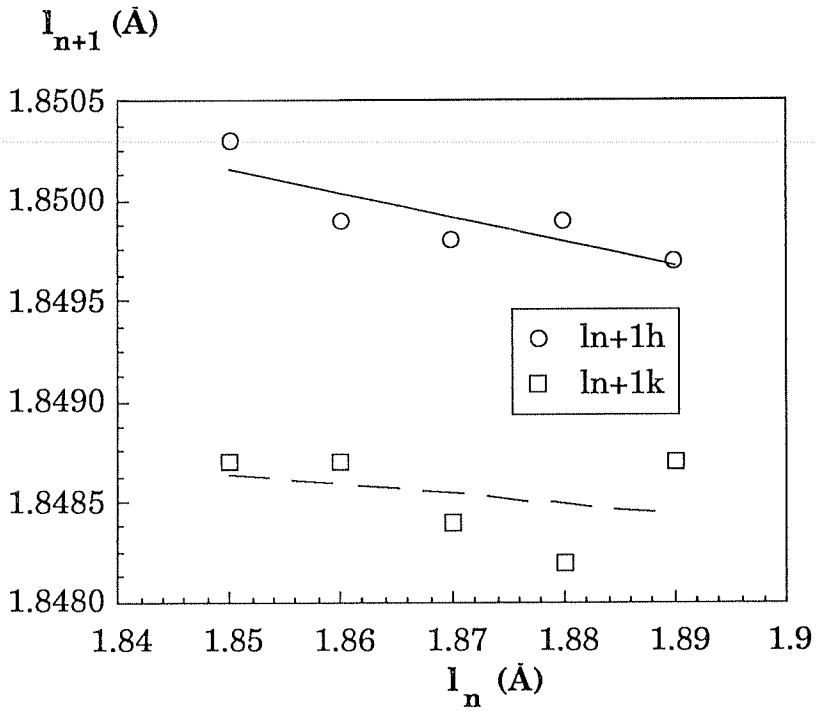

b)

G. L. VIGNOLES & L. DUCASSE

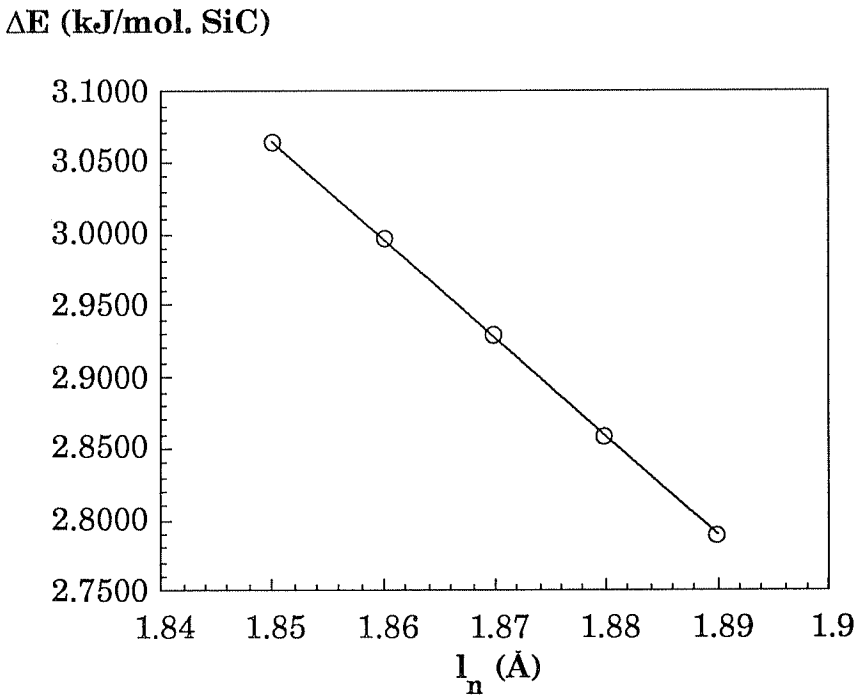

Fig. 10.

G. L. VIGNOLES & L. DUCASSE

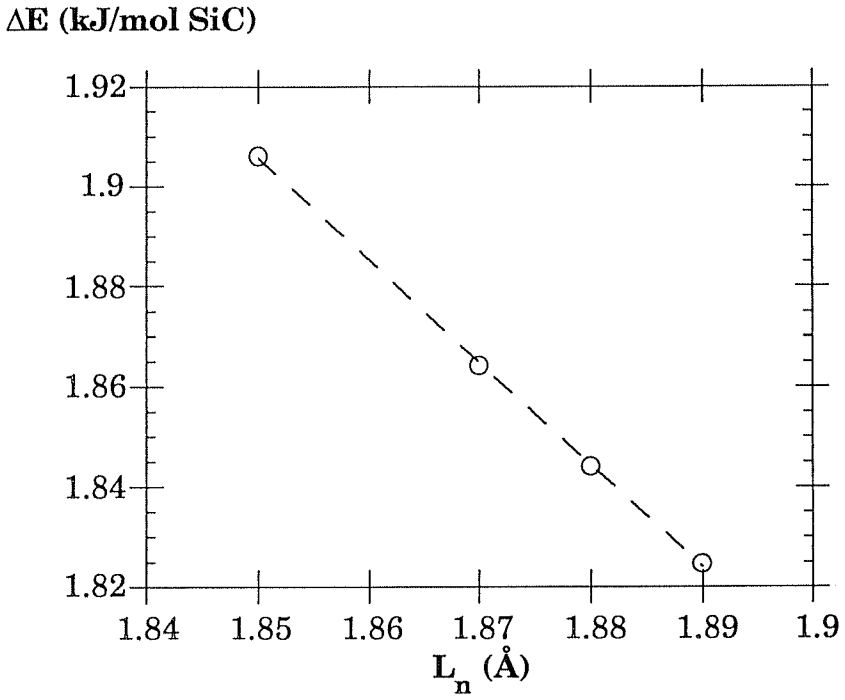

Fig. 11.

G. L. VIGNOLES & L. DUCASSE

Fig. 12.

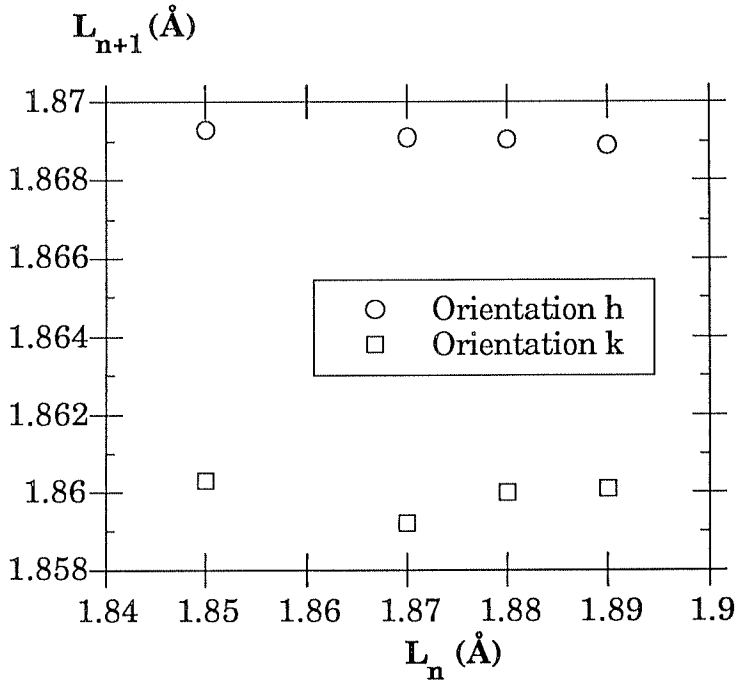

a)

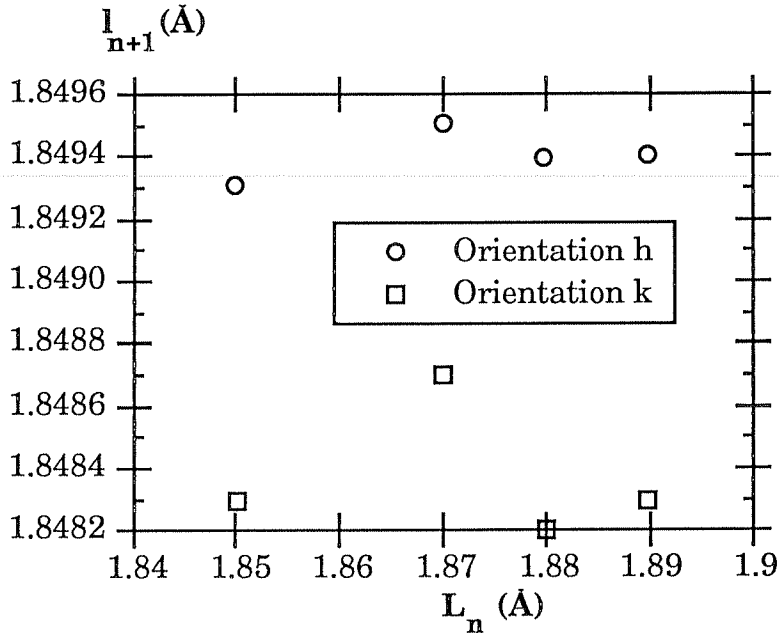

b)

G. L. VIGNOLES & L. DUCASSE

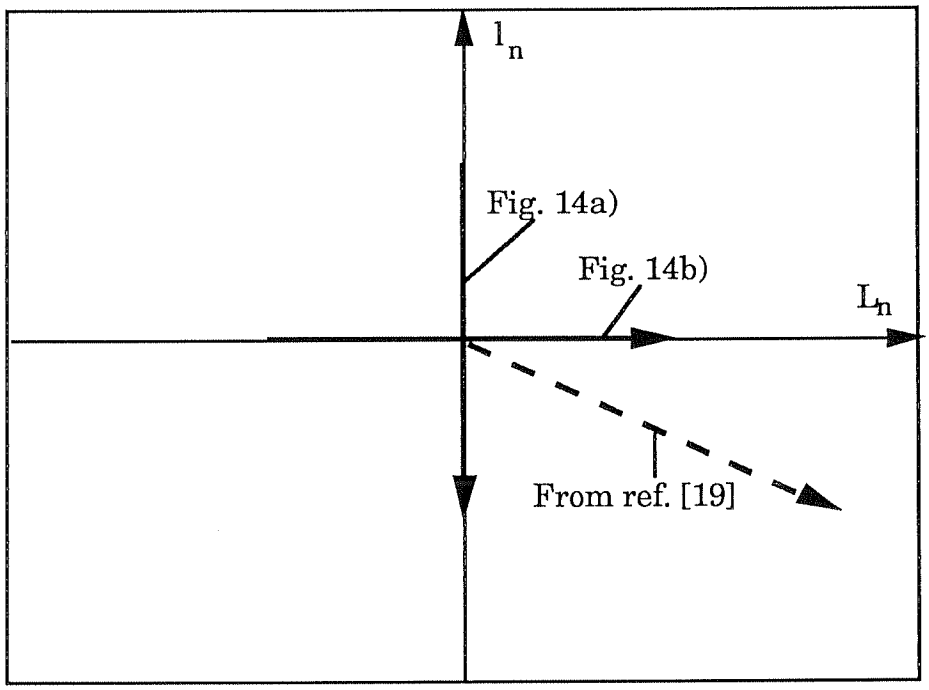

Fig. 13.

G. L. VIGOLES & L. DUCASSE

Fig. 14.

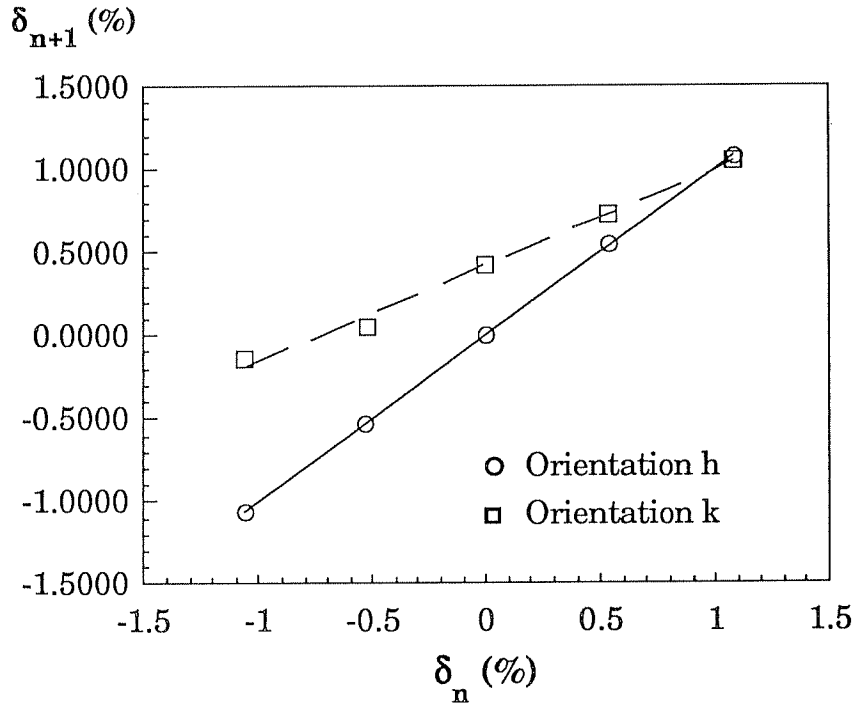

a)

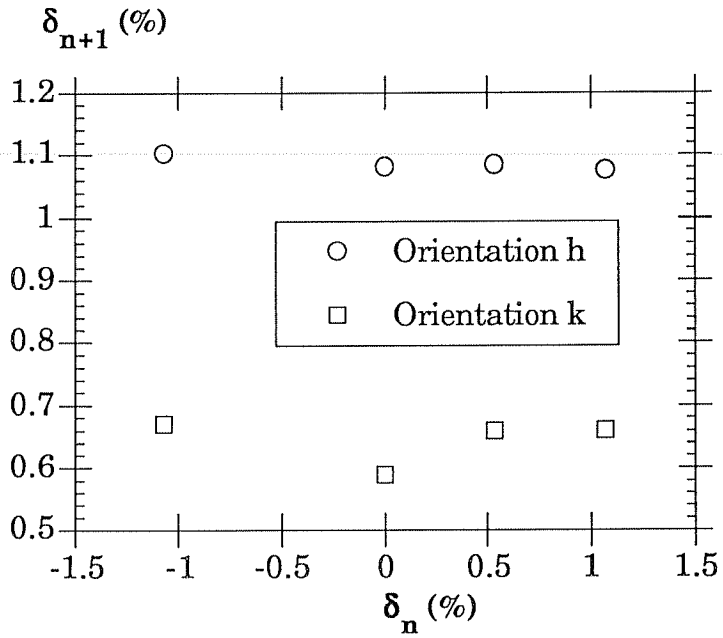

b)

G. L. DIGNOCES & L. DACASSE